

PACS numbers: 52.38.Kd; 52.50.Jm; 42.65.Re
DOI: 10.1070/QE2013v043n03ABEH015100

Generation of quasi-monochromatic beams of accelerated electrons during interaction of weak-contrast intense femtosecond laser radiation with a metal-foil edge

Yu.A. Malkov, A.N. Stepanov, D.A. Yashunin, L.P. Pugachev, P.R. Levashov, N.E. Andreev, A.A. Andreev

Abstract. **The formation of monoenergetic beams of accelerated electrons by focusing femtosecond laser radiation with an intensity of 2×10^{17} W cm^{-2} onto an edge of aluminium foil has been experimentally demonstrated. The electrons had energy distributions peaking in the range from 0.2 to 0.8 MeV and an energy spread less than 20 %. The acceleration mechanism related to the generation of a plasma wave as a result of self-modulation instability of the laser pulse in the subcritical plasma formed the prepulse of the laser system (arriving 10 ns before the main pulse) is considered. One-dimensional PIC simulation of the interaction between the laser radiation and plasma with a concentration of 5×10^{19} cm^{-3} showed that effective excitation of a plasma wave, as well as the trapping and acceleration of the electron beam with an energy on the order of 1 MeV, may occur in the presence of inhomogeneities in the density at the plasma boundary and in the temporal shape of the beam.**

Keywords: *femtosecond laser radiation, acceleration of electrons, self-modulation instability, plasma wave.*

1. Introduction

Acceleration of particles upon excitation of plasma waves by high-intensity subpicosecond laser radiation [1, 2] is a promising field of research in high-energy physics. The immense accelerating fields, exceeding those yielded by standard high-frequency accelerators by several orders of magnitude, make it possible to design compact charged-particle accelerators for different applications in fundamental science, medicine, and diagnostics of extreme states of matter.

One of the key problems in laser-plasma acceleration is the trapping of electrons by an accelerating plasma wave. Recently the so-called bubble electron acceleration in a plasma wave has been actively investigated. In this regime a highly nonlinear plasma wave can trap electrons from the cold background plasma [3]. The self-trapping conditions in this regime were thoroughly investigated in [4, 5]. Many different schemes of electron injection into the accelerating wake wave were proposed: use of a pair of counterpropagating beams [6]; sharp laser beam focusing [7]; laser pulse chirping [8]; use of a mixture of gases, one of which has a high ionisation threshold [9–11]; application of a strong external magnetic field [12]; and formation of various transverse inhomogeneities [13].

At the same time, the studies on acceleration of electrons in a more stable, weakly linear plasma wave are under way. Under these conditions, in contrast to the bubble regime, the electron trapping energy thresholds are much higher due to the low plasma-wave amplitude; thus, the problem of electron injection into the plasma wave is especially urgent. In fact, it has not been solved to date. Although the excitation of weakly linear plasma waves at long paths, which are necessary to accelerate particles to several hundreds of MeV, was demonstrated in [14, 15], there are only few results on synchronous (with the laser pulse) electron injection into the wave.

In some studies there were attempts to inject electrons using an external high-frequency accelerator. However, this scheme proved to be low-efficient because of the difficulties with synchronising the electron beam and laser pulse and the relatively long path of the accelerator electron beam. Currently, an injector based on an RF accelerator, the photocathode of which receives a femtosecond pulse exactly synchronised with the strong pulse exciting a plasma wave [16], is being actively developed; however, practical results have not been published yet.

An alternative way to form a synchronised electron source is to focus high-intensity radiation on a solid. To apply an electron source as an injector to the accelerating wake wave, one must know such characteristics as the degree of collimation and energy homogeneity of the electron beam. Emission of electron beams in the specular direction at focusing laser radiation on the solid target surface at a certain angle was observed in [17–20]. In some experiments the energy spectrum of the electrons emitted from the plasma at a large angle of incidence of laser beam on the solid target surface contained quasi-monoenergetic bunches of accelerated electrons [21, 22]. It was shown that a critically important factor in this case is the existence of pre-plasma, which is induced by the relatively low contrast of laser pulse.

The main specific feature of this study is that laser radiation was focused on the edge of an aluminium foil perpendicular to its plane, so as to ensure free bypass of the foil for some part of laser radiation. We revealed generation of highly collimated electron beams, propagating in the same direction as the laser pulse and characterised by a narrow energy distribution peaking in the range of 0.2–0.8 MeV. The electron-beam charge ranges from 1 to 10 pC.

Yu.A. Malkov, A.N. Stepanov, D.A. Yashunin Institute of Applied Physics, Russian Academy of Sciences, ul. Ul'yanova 46, 603950 Nizhnii Novgorod, Russia; e-mail: yashuninda@yandex.ru;
L.P. Pugachev, P.R. Levashov, N.E. Andreev Joint Institute of High Temperatures, Russian Academy of Sciences, Izhorskaya ul. 13, Bld. 2, 125412 Moscow, Russia; e-mail: pugachev@ihed.ras.ru;
A.A. Andreev Federal State Unitary Enterprise "Scientific and Industrial Corporation 'Vavilov State Optical Institute'", Birzhevay liniya 12, 199034 St. Petersburg, Russia

Received 24 December 2012
Kvantovaya Elektronika **43** (3) 226–231 (2013)
Translated by Yu.P. Sin'kov

2. Experimental technique

The experiment was performed using a Ti:sapphire laser, generating 60-fs pulses with a maximum energy up to 100 mJ and a centre wavelength of 800 nm. The laser beam was focused (using a spherical mirror with a focal length $F = 50$ cm) on the edge of an aluminium 200-μm-thick foil perpendicular to its surface in a vacuum camera (Fig. 1). The maximum intensity in the focus (at a beam radius $r_0 = 25$ μm at a level of $1/e^2$ and a pulse energy of 100 mJ) was $I = 2 \times 10^{17}$ W cm^{-2}. Nonidealities of the polarisation elements of the laser system led to the presence of a prepulse, arriving before the main pulse by 12 ns; it had energy of 10^{-4} of the main pulse energy and was approximately of the same duration. As a result, when focused on the target, the laser intensity in the prepulse exceeded the ionisation threshold for the target material, and the main laser pulse interacted with not only the metal but also with the plasma formed by the prepulse (Fig. 1, inset).

Diagnostics of electrons was performed by recording the luminescence of a Lanex Medium scintillation screen (Kodak) using a Hamamatsu C8484-05G digital camera, equipped with a 25 mm $F/1.4$ objective; the camera was mounted at a distance of 22 cm from the screen. The scintillation screen was isolated from optical radiation using a 10-μm-thick aluminium foil, pressed closely to the screen surface. The data of [23] were used to calculate the sensitivity of the diagnostics for electrons with different energies. The minimum measured electron energy (energy cutoff), with the scintillation-screen sensitivity and the transmittance of the aluminium foil taken into account, was about 140 keV.

A helium–neon laser was used to align the intense laser beam with the target. The laser beam transmitted through the target after the interaction was monitored by recording an enlarged beam image with another CCD camera. The electron energy was measured using a magnetic spectrometer based on a pair of NdFeB magnets, positioned in a magnetic circuit 5 cm in diameter; the uniform magnetic field in the gap was 0.2 kG. Using the luminescence data from the screen, with allowance for its sensitivity in the presence of a foil in front of it, we calculated the electron trajectory and reconstructed the energy spectrum of electrons. A metal slit was placed at the spectrograph input to collimate the electron beam.

A laser pulse was focused by a spherical mirror on the aluminium foil edge so that approximately a half of laser beam fell on the foil and the other half passed by. The foil plane was oriented perpendicular to the laser beam direction. The foil was displaced in two coordinates using a pair of motorised translators.

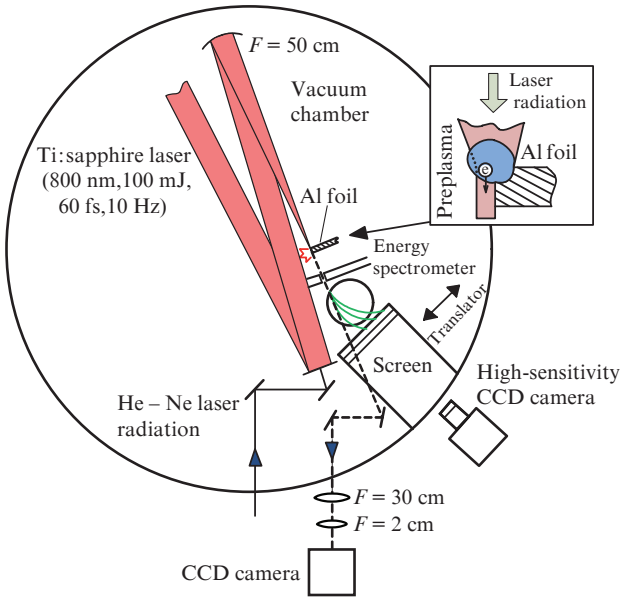

Figure 1. Schematic of the experimental setup. The inset shows the geometry of interaction of the laser pulse and foil.

3. Experimental results

The spatial distribution of accelerated electrons was studied without a magnetic spectrometer. The foil (retained immobile) was successively irradiated with several laser pulses.

We observed luminescence on the scintillation screen; its spatial distribution was controlled for each laser pulse. After the irradiation of a given point on the foil surface by four or five laser pulses the screen luminescence disappeared. A visual analysis showed formation of a through hole about 100 μm in diameter at the interaction point, as a result of which the laser beam passed without distortions through the foil. Then the sample was shifted, and the procedure was repeated on a new portion of the foil edge.

The spatial distribution of the scintillation screen luminescence for most of laser pulses was found to correspond to single highly collimated electron beams with an angular divergence of about 0.5 – 1°, directed close to the laser beam propagation direction (Fig. 2). The beams were surrounded by weak uniform luminescence.

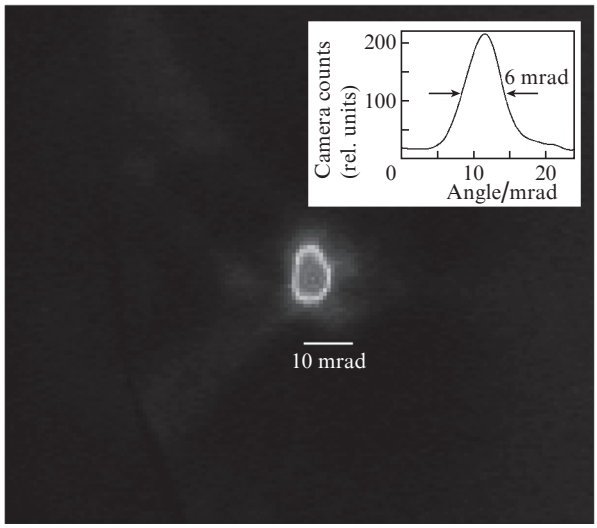

Figure 2. Angular distribution of the electron beam formed by focusing laser radiation onto the foil edge.

The energy spectrum of spatially collimated beams was measured on a magnetic spectrograph with an input slit located before the scintillation screen. The beam spectrum was found to have a nonmonotonic energy distribution with one or several peaks. A single energy peak with an FWHM less than 20% of the maximum energy was observed for some laser pulses. The luminescence patterns on the screen for two

such laser pulses (A and B) are shown in Fig. 3, with indication of the electron energy values corresponding to the deviation of electrons and the boundaries of the projection of the spectrograph input slit on the screen. The normalised energy spectra of electrons, found from the spatial distribution of the screen luminescence, are shown in Fig. 4 (curves A and B). An energy spectrum of electrons with several peaks was observed for some laser pulses (Fig. 4, curve C). The spectra presented correspond to laser pulse energies in the range of 60–80 mJ.

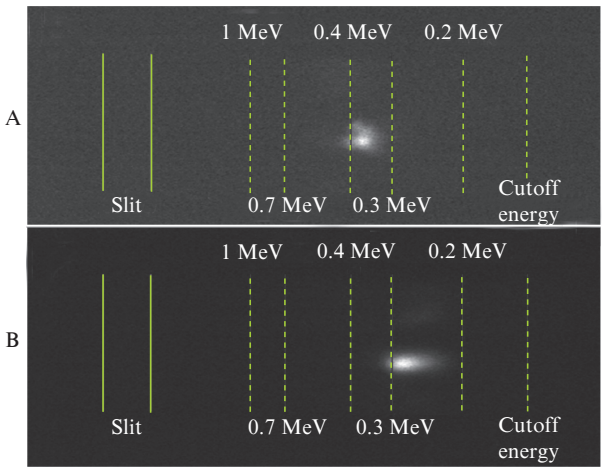

Figure 3. Distribution scintillation screen luminescence on the CCD camera for two laser pulses (A, B).

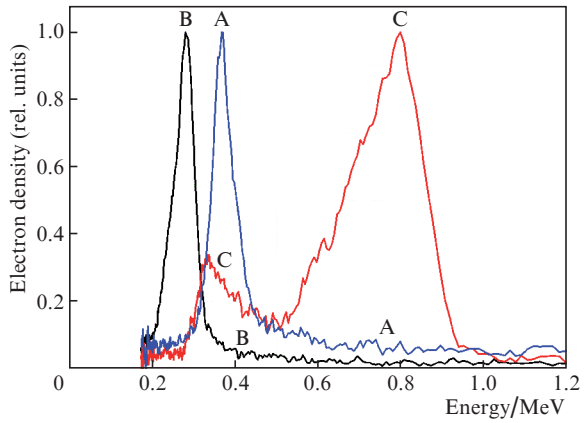

Figure 4. Experimental electron energy spectra (beams A, B, and C) for three different laser pulses.

Note that the slit of the electron spectrometer is wider than the electron beam cross section; therefore, the energy resolution is determined by the beam sizes, and the peaks in the energy distribution may be narrower in reality. As follows from these data, the electron energy peaks lie in the range from 0.2 to 0.8 MeV.

4. Theoretical description

One of possible mechanisms of the formation of accelerated electrons with a quasi-monochromatic spectrum is the acceleration in the field of the plasma wave generated in the prepulse-induced dense plasma due to the self-modulation of laser-pulse instability [24]. On the assumption that the prepulse arriving approximately 10 ns before the main pulse and having an intensity $I \sim 10^{13}$ W cm^{-2} ionises the target metal at the skin depth, after which the thus formed plasma spreads with ion sound velocity, the plasma density is in the range of 10^{19}–10^{20} cm^{-3}, and the characteristic plasma size by the time of the main pulse arrival is ~100 μm. When a laser pulse propagates in this dense plasma, the length of the wake plasma wave, $\lambda_p = 2\pi c/\omega_p$, is much shorter than that of the femtosecond pulse ($L = c\tau_L$), which may lead to its self-modulation and effective generation of accelerating wake field. We should emphasise the following: the development of self-modulation instability and generation of wake field by a relatively long laser pulse ($L \gg \lambda_p$) requires a sufficiently large initial amplitude of the 'seed' plasma wave and propagation of the laser pulse by a rather long distance [25].

To analyse the wake acceleration of electron bunches, we performed a pilot particle-in-cell (PIC) simulation in one-dimensionally inhomogeneous (1D3V) plasma. The simulation was performed using the 1D version of the VLPL code [26]. A laser pulse with a width $\tau_L = 66$ fs propagated along the x axis. The pulse had a transverse linear polarisation along the y axis. The laser pulse wavelength $\lambda = 1$ μm and the dimensionless amplitude $a_0 = eE/(m_e c\omega) = 0.468$, where e is the elementary charge, m_e is the electron mass, c is the speed of light, and ω is the laser frequency; these parameters correspond to the intensity $I_0 = 3 \times 10^{17}$ W cm^{-2}. The size of the simulation region is $L = 160$ μm. At the initial instant the laser-pulse centre is at $x = 0$. In the region $0 \leqslant x < 40$ μm the plasma has an inhomogeneously increasing (Gaussian or linear) density profile with a characteristic inhomogeneity size $l = 15$ μm. At 40 μm $< x \leqslant 160$ μm the plasma is homogeneous with a density $n_0 = 0.045 n_{cr} = 5 \times 10^{19}$ cm^{-3}, where $n_{cr} = m_e\omega^2/(4\pi e^2)$ (Fig. 5, dotted line). The cell size $\Delta x = 0.01$ μm and the number of particles per cell is 500. The ions were

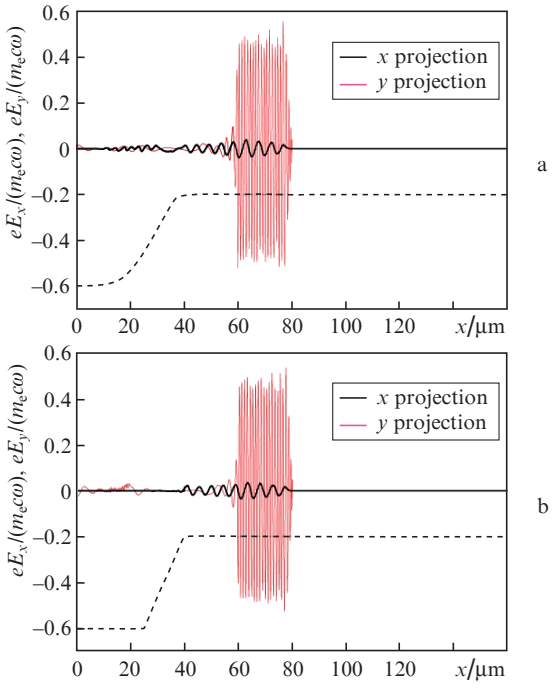

Figure 5. Dimensionless projections of the electric field vector at t = 233 fs (ct = 70 μm) for (a) Gaussian and (b) linear density profiles. The plasma density profiles are shown by dashed curves.

assumed to be immobile and form a neutralizing background. At the initial instant the plasma was considered cold.

The calculations performed with a Gaussian time profile of the laser pulse showed the following: for the plasma and pulse parameters, when the pulse has a smooth envelope and relatively low intensity, the 'seed' plasma-wave amplitude is insufficiently large to develop a self-modulation instability and generate an accelerating wake field.

The generation of a wake wave and acceleration of electrons in it occur differently in the case of sharp leading edge of a rectangular (or hyper-Gaussian) laser pulse (Figs 5–8). Note that the pulse leading edge may be sharpened under experimental conditions due to the ionisation nonlinearity [27]. Figures 5–8 show the calculation results for Gaussian and linear profiles of plasma density with a characteristic inhomogeneity size l = 15 μm at the input of plasma layer.

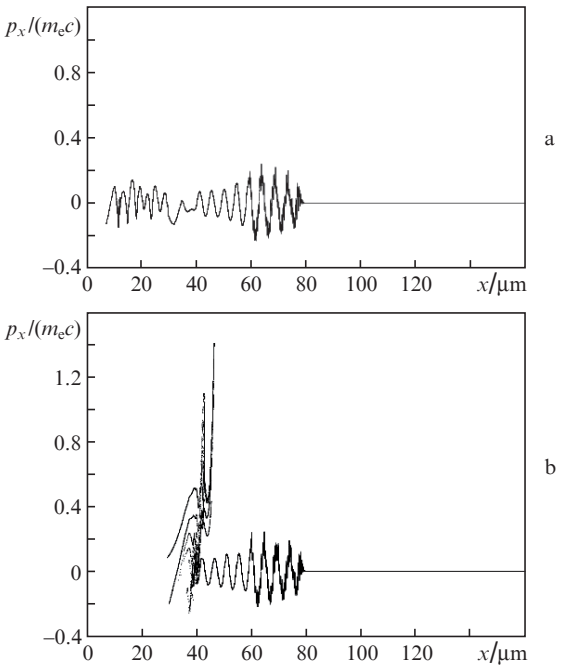

Figure 6. Phase plane of electrons at t = 233 fs (ct = 70 μm) for (a) Gaussian and (b) linear plasma density profiles.

As can be seen in Figs 5 and 7, while the laser pulse propagates in the plasma layer, the pulse self-modulation and generation of a wake wave are independent of the plasma density profile at the layer input. However, the phase space images (Fig. 6) show that the dynamics of a small part of electrons in the region of the sharp change in the spatial distribution of the plasma density at the layer input (in the case of linear profile) radically differs from the case of smooth Gaussian density profile, which passes to the homogeneous layer without jumps in the derivative.

Due to the sharp change in the wave phase velocity [28], a small part of electrons trapped by the wake wave at the boundary of homogeneous plasma layer (Fig. 6b) acquire a rather high energy as a result of acceleration in the rising (during the development of laser pulse self-modulation) wake wave (Fig. 8b). The corresponding electron energy spectrum is shown in Fig. 9 on the logarithmic (to energy of ~5 MeV) and linear (to energy of 1 MeV) scales.

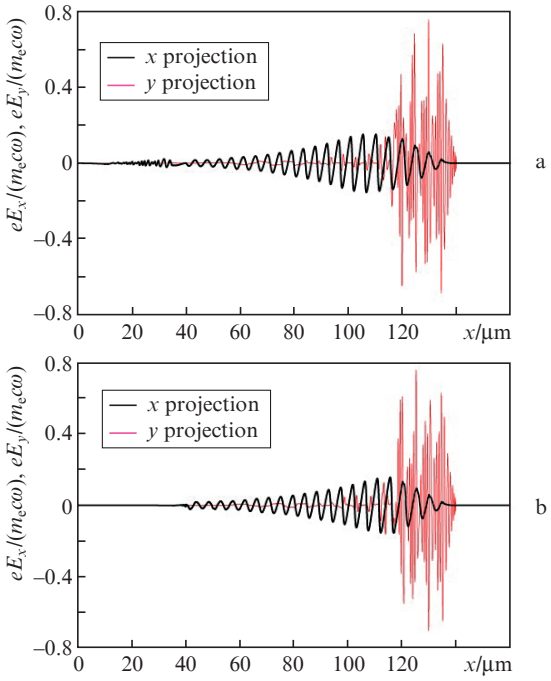

Figure 7. Dimensionless projections of the electric field vector at t = 433 fs (ct = 130 μm) for (a) Gaussian and (b) linear density profiles.

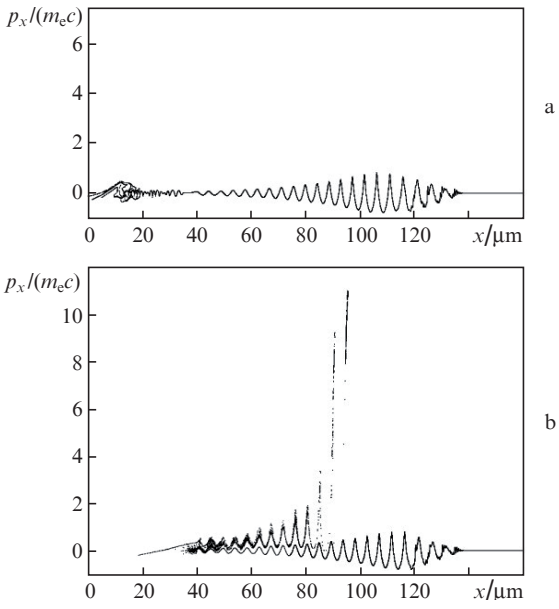

Figure 8. Phase plane of electrons at t = 433 fs (ct = 130 μm) for (a) Gaussian and (b) linear plasma density profiles.

Figure 9a shows the electron spectrum in the entire range of acceleration energies (about 5 MeV; see Fig. 8b). Several groups of accelerated electrons are observed. However, the number of accelerated electrons with energies exceeding 0.6 MeV is much smaller than the number of electrons in the main maximum of distribution of accelerated electrons with energies from 0.5 to 0.6 MeV. This can clearly be seen in Fig. 9b, which also demonstrates another pronounced peak near ~0.3 MeV. The formation of several groups of accelerated electrons is due to the trapping and acceleration of electrons in different periods of the wake plasma wave (Fig. 8b).

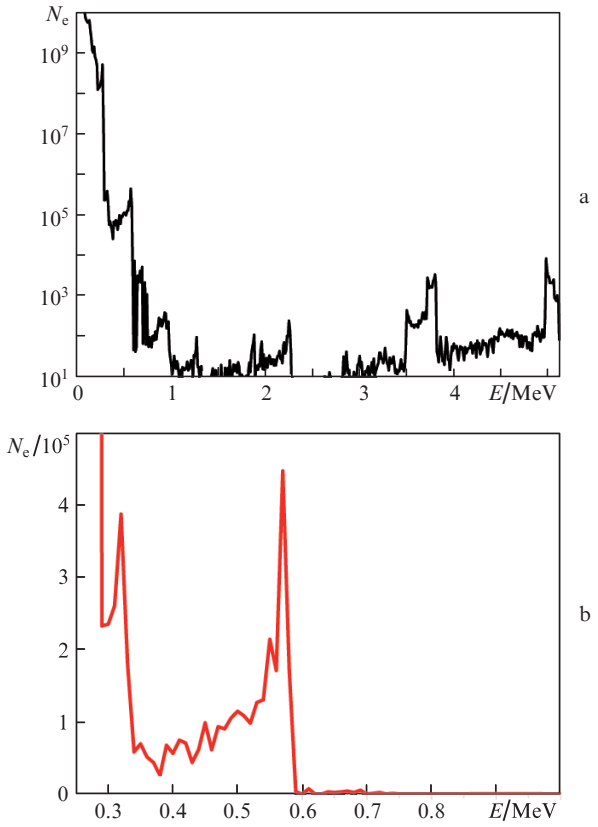

Figure 9. Energy spectra of electrons at $t = 433$ fs ($ct = 130$ μm) on the (a) logarithmic and (b) linear scales for a linear plasma density profile at the input of the layer. The number of electrons per transverse (with respect to the x axis) cross section with an area $\lambda^2 = 1$ μm^2 per unit energy (in MeV) is plotted on the vertical axes.

The simulation results (Figs. 8, 9) indicate that the wake mechanism of acceleration and formation of directed high-energy electron bunches can be implemented under our experiment (see Fig. 4). The necessary condition is the presence of a sharply changing profile of plasma density at the input of the plasma layer formed by the laser prepulse or a sufficiently sharp leading edge of the laser pulse, which may arise as a result of ionisation nonlinearity when the main femtosecond laser pulse propagates in the incompletely ionised plasma formed by the prepulse. The charge of accelerated electrons in the quasi-monoenergetic bunch with energies from 0.5 to 0.6 MeV (Fig. 9b), emitted from an area determined by the laser beam focus spot with a radius $r_0 \approx 25$ μm, is 5 pC; i.e., it is in the range of experimentally measured values. Note that the possibility of using one-dimensionally inhomogeneous (along the laser beam propagation direction) model of plasma in the pilot one-dimensional (1D3V) PIC simulation of experimental results is due to the relatively large characteristic size of transverse plasma inhomogeneity by the instant of the main pulse arrival (~100 μm) in comparison with the radius of laser beam focus spot (which determines the characteristic transverse size of the wake wave, which accelerates electrons).

5. Conclusions

In this paper, we report the results of experimental and theoretical study of a fast-electron source, which can be used for injection in schemes of laser-plasma acceleration of electrons in a plasma wave [14, 15]. The experiment on irradiation of an aluminium foil edge by a focused high-intensity femtosecond laser beam showed generation of highly collimated quasi-monochromatic electron beams, whose direction coincided with the laser beam propagation direction. The electron energy in the energy distribution peak was 0.2–0.8 MeV, with the peak width smaller than 20%; the beam divergence was 0.5–1°.

The high directionality of the electron beam and its narrow energy spectrum can be explained by the acceleration of electrons in the plasma wave, which is generated as a result of self-modulation instability of intense laser pulse in the plasma formed by the prepulse arriving at the target about 10 ns before the main pulse. The results of one-dimensional (1D3V) PIC simulation of the interaction of laser radiation with dense subcritical plasma were presented. The simulation showed that effective excitation of a plasma wave, as well as the trapping and acceleration of electron beams with energies of about 1 MeV, may occur in the presence of inhomogeneities at the plasma boundary and in the time envelope of the beam. Under our experimental conditions the inhomogeneities in the temporal structure of the beam may be caused by ionisation nonlinearity of the plasma formed by the prepulse, and the spatial density inhomogeneities may be due to the sharp boundaries of the foil and the complex configuration of the plasma spread.

We plan to analyse (with the aid of completely three-dimensional PIC simulation) the influence of plasma transverse inhomogeneity on the acceleration of electron bunches. This simulation will make it possible to perform a more detailed comparison of the theoretical predictions with the experimental results and optimise the generation of low-divergent quasi-monoenergetic electron bunches, which can be used for injection in wake-wave based laser-plasma accelerators.

Acknowledgements. This work was supported by the Russian Foundation for Basic Research (Grant No. 10-02-93121-NTsNIL_a) and the programme 'Extreme Light Fields and Their Applications' of the Presidium of the Russian Academy of Sciences.

References

1. Tajima T., Dawson J.M. *Phys. Rev. Lett.*, **43**, 267 (1979).
2. Esarey E., Schroeder C.B., Leemans W.P. *Rev. Mod. Phys.*, **81**, 1229 (2009).
3. Pukhov A., Meyer-ter-Vehn J. *Appl. Phys. B*, **74**, 355 (2002).
4. Mangles S.P.D., Genoud G., Bloom M.S., Burza M., Najmudin Z., Persson A., Svensson K., Thomas A.G.R., Wahlström C.G. *Phys. Rev. Spec. Top. – Accel. Beams*, **15**, 011302 (2012).
5. Ma Y.Y., Kawata S., Yu T.P., Gu Y.Q., Sheng Z.M., Yu M.Y., Zhuo H.B., Liu H.J., Yin Y., Takahashi K., Xie X.Y., Liu J.X., Tian C.L., Shao F.Q. *Phys. Rev. E*, **85**, 046403 (2012).
6. Faure J., Rechatin C., Norlin A., Lifschitz A., Glinec Y., Malka V. *Nature*, **444**, 737 (2006).
7. Xu H., Yu W., Lu P., Senecha V.K., He F., Shen B., Qian L., Li R., Xu Z. *Phys. Plasmas*, **12**, 013105 (2005).
8. Pathak V.B., Vieira J., Fonseca R.A., Silva L.O. *New J. Phys.*, **14**, 023057 (2012).
9. Pollock B.B., Clayton C.E., Ralph J.E., Albert F., Davidson A., Divol L., Filip C., Glenzer S.H., Herpoldt K., Lu W., Marsh K.A., Meinecke J., Mori W.B., Pak A., Rensink T.C., Ross J.S., Shaw J., Tynan G.R., Joshi C., Froula D.H. *Phys. Rev. Lett.*, **107**, 045001 (2011).
10. Liu J.S., Xia C.Q., Wang W.T., Lu H.Y., Wang C., Deng A.H., Li W.T., Zhang H., Liang X.Y., Leng Y.X., Lu X.M., Wang C.,

Wang J.Z., Nakajima K., Li R.X., Xu Z.Z. *Phys. Rev. Lett*., **107**, 035001 (2011).
11. Ho Y.C., Hung T.S., Yen C.P., Chen S.Y., Chu H.H., Lin J.Y., Wang J., Chou M.C. *Phys. Plasmas*, **18**, 063102 (2011).
12. Vieira J., Martins S.F., Pathak V.B., Fonseca R.A., Mori W.B., Silva L.O. *Phys. Rev. Lett*., **106**, 225001 (2011).
13. Shen B., Li Y., Nemeth K., Shang H., Chae Y.-c., Soliday R., Crowell R., Frank E., Gropp W., Cary J. *Phys. Plasmas*, **14**, 053115 (2007).
14. Wojda F., Cassou K., Genoud G., Burza M., Glinec Y., Lundh O., Persson A., Vieux G., Brunetti E., Shanks R.P., Jaroszynski D., Andreev N.E., Wahlström C.G., Cros B. *Phys. Rev. E*, **80**, 066403 (2009).
15. Eremin V., Malkov Y., Korolikhin V., Kiselev A., Skobelev S., Stepanov A., Andreev N. *Phys. Plasmas*, **19**, 093121 (2012).
16. Stragier X.F.D., Luiten O.J., van der Geer S.B., van der Wiel M.J., Brussaard G.J.H. *J. Appl. Phys*., **110**, 024910 (2011).
17. Bastiani S., Rousse A., Geindre J.P., Audebert P., Quoix C., Hamoniaux G., Antonetti A., Gauthier J.C. *Phys. Rev. E*, **56**, 7179 (1997).
18. Sentoku Y., Ruhl H., Mima K., Kodama R., Tanaka K.A., Kishimoto Y. *Phys. Plasmas*, **6**, 2855 (1999).
19. Chen L.M., Zhang J., Li Y.T., Teng H., Liang T.J., Sheng Z.M., Dong Q.L., Zhao L.Z., Wei Z.Y., Tang X.W. *Phys. Rev. Lett*., **87**, 225001 (2001).
20. Wang W., Liu J., Cai Y., Wang C., Liu L., Xia C., Deng A., Xu Y., Leng Y., Li R., Xu Z. *Phys. Plasmas*, **17**, 023108 (2010).
21. Mordovanakis A.G., Easter J., Naumova N., Popov K., Masson-Laborde P.-E., Hou B., Sokolov I., Mourou G., Glazyrin I.V., Rozmus W., Bychenkov V., Nees J., Krushelnick K. *Phys. Rev. Lett*., **103**, 235001 (2009).
22. Mao J.Y., Chen L.M., Ge X.L., Zhang L., Yan W.C., Li D.Z., Liao G.Q., Ma J.L., Huang K., Li Y.T., Lu X., Dong Q.L., Wei Z.Y., Sheng Z.M., Zhang J. *Phys. Rev. E*, **85**, 025401 (2012).
23. Glinec Y., Faure J., Guemnie-Tafo A., Malka V., Monard H., Larbre J.P., De Waele V., Marignier J.L., Mostafavi M. *Rev. Sci. Instrum*., **77**, 103301 (2006).
24. Andreev N.E., Gorbunov L.M., Kirsanov V.I., Pogosova A.A., Ramazashvili R.R. *Physica Scripta*, **49**, 101 (1994).
25. Andreev N.E., Kirsanov V.I., Gorbunov L.M. *Phys. Plasmas*, **2**, 2573 (1995).
26. Pukhov A. *J. Plasma Phys*., **61**, 425 (1999).
27. Andreev N.E., Chegotov M.V., Pogosova A.A. *Zh. Eksp. Tekh. Fiz*., **123**, 1006 (2003).
28. Bulanov S.V., Inovenkov I.N., Naumova N.M., Sakharov A.S. *Fiz. Plazmy*, **16**, 764 (1990).